OPTIMIZATION OF TIN HALIDE PEROVSKITE SOLAR CELL USING TAGUCHI METHOD

NURUL ATIKAH BINTI MOHD MAZLAN

UNIVERSITI TEKNIKAL MALAYSIA MELAKA

OPTIMIZATION OF TIN HALIDE PEROVSKITE SOLAR CELL USING TAGUCHI METHOD

NURUL ATIKAH BINTI MOHD MAZLAN

This report is submitted in partial fulfilment of the requirements for the degree of Bachelor of Electronic Engineering with Honours

Faculty of Electronic and Computer Technology and Engineering
Universiti Teknikal Malaysia Melaka

2023/2024

DECLARATION

I declare that this report entitled "OPTIMIZATION OF TIN HALIDE PEROVSKITE SOLAR CELL USING TAGUCHI METHOD" is the result of my own work except for quotes as cited in the references.

Signature : .....

Author : NURUL ATIKAH MOHD MAZLAN .....

Date : 27 JUN 2024 .....

APPROVAL

I hereby declare that I have read this thesis and in my opinion this thesis is sufficient in terms of scope and quality for the award of Bachelor of Electronic Engineering with Honours.

Signature : .....

Supervisor Name : Prof. Madya Ir. Dr. Fauziyah binti Salehuddin

Date : 27 June 2024

DEDICATION

First and foremost, I am very grateful to all the family members for their valuable guidance and support in the completion of this project in its entirety. I would like to express our deepest appreciation to all those who provided us the possibility to complete our Integrated Design Project. A special gratitude I give to my supervisor, Prof. Madya Ir. Dr. Fauziyah Binti Salehuddin and co supervisor Ts. Dr. Faiz Bin Arith whose contribution in stimulating suggestions and encouragement and help me a lot in this project and with much appreciation too because she and he gave the knowledge about this project to use all required equipment and the necessary materials to complete the project. Next, I also appreciate the guidance given by panels that have improved our project and the knowledge that gives us the idea to complete this project. Finally, gratitude goes to all my friends who directly or indirectly helped me to complete this project.

ABSTRACT

In the realm of photovoltaics, tin halide perovskite solar cells have emerged as promising candidates for efficient and cost-effective energy conversion. This project investigates a comprehensive analysis of tin halide perovskite solar cell models using Solar Cell Capacitance Simulator- One Dimensional (SCAPS-1D). The main goal of this project is to optimize the performance of the solar cell and for this purpose, the Taguchi method is employed. Parameter variation can be minimized and important factors can be identified with the help of this method. In order to attain reduced variance with ideal control parameter values, it uses an orthogonal array (OA) experiment. An efficiency of 26.24% has been achieved by tin halide in PSC, according to simulations using SCAPS-1D. Following Taguchi Method L9 OA optimization, the efficiency improved to 27.11%. This shows that the Taguchi Method was successful in predicting the ideal solution for reaching the required efficiency in PSC device. Overall, the study shows that the Taguchi Method can be used to optimize tin halide and increase PSC efficiency.

ABSTRAK

Dalam bidang fotovoltaik, sel solar perovskite timah halida telah muncul sebagai calon yang menjanjikan untuk penukaran tenaga yang cekap dan kos-efektif. Projek ini menyelidiki analisis komprehensif model sel solar perovski timah halida, menggunakan Simulator Kapasitans Sel Suria-Satu Dimensi (SCAPS-1D). Matlamat utama adalah untuk mengoptimumkan prestasi sel suria ini dan bagi tujuan ini, kaedah Taguchi digunakan. Variasi parameter boleh diminimumkan dan faktor penting boleh dikenal pasti dengan bantuan kaedah ini. Bagi mencapai varians yang dikurangkan dengan nilai parameter kawalan yang ideal, ia menggunakan percubaan tatasusunan ortogon (OA). Kecekapan 26.24% telah dicapai oleh timah halida dalam PSC, mengikut simulasi menggunakan SCAPS-1D. Berikutan pengoptimuman OA Kaedah Taguchi L9, kecekapan meningkat kepada 27.11%. Ini menunjukkan bahawa Kaedah Taguchi berjaya meramalkan penyelesaian ideal bagi mencapai kecekapan yang diperlukan dalam peranti PSC. Secara keseluruhannya, kajian menunjukkan Kaedah Taguchi boleh digunakan untuk mengoptimumkan timah halida dan meningkatkan kecekapan PSC.

ACKNOWLEDGEMENTS

First and foremost, all praises be to Allah S.W.T the most Gracious the most Merciful, for His showers of blessings giving us strength and patient in this study. Throughout the completion of this project, I would like to express my utmost gratitude toward my project supervisor, Prof. Madya Ir. Dr. Fauziyah Binti Salehuddin and my co-supervisor Ts. Dr. Faiz Bin Arith for their germinal ideas, encouragement, guidance, and time throughout the progress of this project. Without their continued support and interest, I could not be able to complete my project successfully.

My deepest gratitude goes to all my family members. All the support that they give to me is the reason where I am now. Without them, I will be lost by myself

TABLE OF CONTENTS

LIST OF FIGURES

LIST OF TABLES

LIST OF SYMBOLS AND ABBREVIATIONS

For examples:

Ti02	:	Titanium Dioxide
ZnO:Al	:	Aluminum doped zinc oxide
PSC	:	Perovskite Solar Cell
SCAPS	:	Solar Cell Capacitance Simulator
Jsc	:	Density of Short Circuit Current
Voc	:	Open Circuit Voltage
FF	:	Fill Factor
PCE	:	Power Conversion Efficiency
S/N	:	Signal to noise
CH3NH3SnI3	:	Methylammonium tin iodide
Au	:	Metal Anode
Cul	:	Cuprous iodide
ETL	:	Electron Transport Layer
HTL	:	Hole Transport Layer

CHAPTER 1

INTRODUCTION

This chapter describe the idea of the Tin Halide Perovskite Solar Cells which includes the background of the project, problem statement, objectives and scope of the project.

1.1 Background

With the increasing modernization in this world, humans are tending to be more dependent on machines, and hence more energy resources are required to satisfy our needs. There are numerous ways to generate electricity, some of which are non-renewable and some of which are renewable, but in recent years, there has been a lot of emphasis on renewable sources because they do not release hazardous gasses or by-products [1]. Solar energy is a well-known renewable energy source that has recently received a lot of attention due to several developments that are making it profitable [2]. The rapid gain in efficiency in such a short period of time is also noteworthy. Since the birth of solar energy, the solar business has seen many different sorts of

devices, the most current of which being Perovskite Solar Cells (PSCs). Photovoltaic cells can directly convert the sun's beams into electricity.

Perovskite halide solar cells are well-known but due to the presence of lead in them, I have to switch to its alternative, Tin-halide Perovskites Solar Cell. In this proposed device, I am using CH3NH3SINI3 instead. Not only is this non-toxic perovskite layer, but it also has many other advantages like a small band gap (1.3eV) and a high absorption coefficient [2]. Due to the combination of layers and their properties, we were able to achieve a highly efficient device. Figure 1.1 shows the required layers of solar cell that will be used in this device.

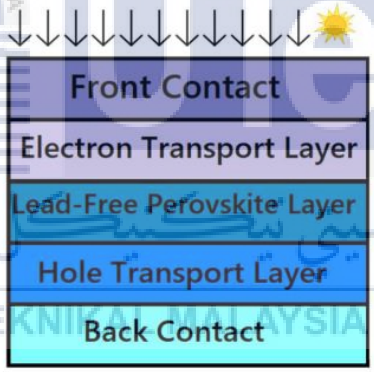

Figure 1.1: Layer used in the simulation of Tin Halide Perovskite Solar Cell

Figure 1.1 shows each playing a specific role in converting sunlight into electricity. At the bottom of the cell lies the front contact, which combines a transparent substrate and a Transparent Conductive Oxide (TCO) layer, providing structural support and enabling the collection and transport of the generated electrical current [3]. Above this is the Electron Transport Layer (ETL), crucial for efficiently extracting and transporting electrons generated when sunlight is absorbed. The lead-free perovskite

layer is the heart of the cell, responsible for light absorption and the generation of electron-hole pairs [4]. This layer is typically composed of a tin-based perovskite material. The Hole Transport Layer (HTL) follows, extracting positively charged holes while preventing recombination with electrons [5]. Lastly, the back contact, the topmost layer, collects the charge carriers and facilitates their exit to the external circuit. These layers collaborate to ensure the effective conversion of sunlight into electricity, and simulations are essential for optimizing their performance and sustainability, advancing Tin Halide Perovskite Solar Cell technology.

The purpose of the Taguchi method is to find factors that are most important in achieving useful goals in a manufacturing process. These factors are varied over two or more levels in a systematic manner. The experiments is designed according to an Orthogonal Array to show the effects of each potential primary factor. The presence of Orthogonal Array (OA) is one of the major advantages of the Taguchi method. Taguchi method also helps in minimizing the number of experiments required in optimization purpose [6].

1.2 Problem Statement

In the domain of renewable energy, tin halide perovskite solar cells are a promising technology due to their potential for highly efficient and cost-effective solar energy conversion [7]. However, their widespread adoption faces critical challenges. These solar cells exhibit impressive efficiency but suffer from stability and long-term performance issues, degrading under real-world conditions and showing variability in efficiency due to factors like material impurities and manufacturing inconsistencies [1]. Existing research has improved efficiency, yet there remains a substantial research gap in achieving the ideal balance between efficiency and long-term stability. A

systematic and optimized approach is needed to enhance efficiency while maintaining stability, along with a deeper understanding of material-related issues and defects. This project addresses these challenges by using SCAPS-1D simulations and the Taguchi method to study and optimize tin halide perovskite solar cells, aiming to develop strategies that boost efficiency and long-term stability, ultimately contributing to the advancement of clean and efficient energy solutions.

1.3 Objective

Specifically, the objectives of the project are:

(i) To design tin halide PSC efficiency by using SCAPS-1D software.

(ii) To optimize the tin halide PSC device using Taguchi approach.

(iii) To analyze the efficiency of perovskite solar cell (PSC) containing tin halide material.

1.4 Scope of work

The scope of work for this project focuses on optimizing tin perovskite solar cells as a clean and efficient energy solution. It encompasses comprehensive simulation and modeling using SCAPS-1D to understand the intricacies of charge carrier dynamics, recombination mechanisms, and material properties in these solar cells [8]. The Taguchi method will be employed for systematic parameter optimization, allowing for the exploration of critical factors like the choice of absorber material, material thickness, defect concentrations, and operating temperature [9]. Experimental validation may be conducted to verify the simulation results and provide real-world insights. Extensive data analysis will be undertaken to identify the most effective parameter combinations for maximizing energy conversion efficiency while maintaining environmental safety. Furthermore, this project aims to develop strategies

for enhancing both the efficiency and long-term stability of tin perovskite solar cells, addressing the challenges associated with lead perovskite materials. The findings will be documented in comprehensive reports, accompanied by future recommendations for research and practical implementation. The project timeline and allocation of necessary resources ensure a systematic and efficient approach to advance the field of clean energy solutions.

1.5 Thesis outline

This thesis consists of five chapters and those are introduction, literature review, methodology, results, and discussion and finally conclusion and recommendation. Each section explains in detail with the depth of this project. The introduction of this project is explained in Chapter 1. In this section explanation of the background, objectives of the project, problem statement, project scope and thesis outline are listed with details. The literature review is described in Chapter 2. The project's research was reviewed in order to compile all key information. In addition, a few initiatives identical to this thesis were researched to ensure a positive outcome. This project's methodology is described in the Chapter 3. This chapter will cover the project activities, which includes the entire design using SCAP-1D software and optimize using L9 OA Taguchi Method. This chapter will go through each simulation design in detail. The results and discussion from this project's simulation are described in Chapter 4. This chapter will explain the results obtained and also analyzed and discussed the results. To obtain a better efficiency, the optimum value based on optimization using Taguchi method need to be obtained. The project's conclusion and recommendations are described in Chapter 5. The entire project and the achievement

of project objectives are concluded in this section. The recommendation is to conduct further study in order to improve the situation.

CHAPTER 2

BACKGROUND STUDY

This chapter provides an overview of theoretical frameworks which includes the previous research on Tin Halide Perovskite Solar Cell.

2.1 Perovskite Solar Cell

Perovskite solar cells (PSCs) have garnered significant interest from researchers worldwide due to their exceptional power conversion efficiency (PCE), cost-effective materials, and straightforward manufacturing process. These solar cells, which follow the formula ABX3 [A = FA (NH2CH=NH2), MA (CH3NH3); B = Pb2; X = Cl, Br, or I], where X represents a halide, possess a crystal structure similar to that of calcium titanite (CaTiO3).

There are two main categories of halide perovskites which organic-inorganic halide-based perovskites and alkali halide-based perovskites. Organic-inorganic halide-based perovskites contain organic monovalent cations (A) such as CH3NH3,

$CH_3CH_2NH_3$, NH_2CHNH_2, and divalent cations (B) like Pb, Sn, Ge, along with halogens (X) such as Cl, Br, I, and F. On the other hand, alkali halide-based perovskites include monovalent alkali cations (A) like Cs, Rb, K, Na, and Li, and divalent cations (B) such as Pb, Sn, Ge, and halogens (X) including Cl, Br, I, and F. These materials are at the forefront of photovoltaic technology due to their exceptional optical and electrical properties. Key features include a high absorption coefficient, tunable band gap, long diffusion length, minimal carrier recombination loss, and high carrier mobility.

The unique properties of perovskites allow for the creation of semitransparent solar cells, where part of the light is absorbed by the light-harvesting layer and the rest passes through. The ability to tune the band gap enables control over transparency by adjusting the thickness of the perovskite layer. The initial photovoltaic device based on lead halide perovskite achieved an efficiency of 2.2%, as demonstrated by Miyasaka using $CH_3NH_3PbBr_3$. This efficiency was later improved to 3.8% by replacing bromine with iodine. The introduction of spiro-MeOTAD as a hole-transporting material further increased efficiency to 9.7% in the first solid-state perovskite solar cells. Through advancements in thin film deposition and perovskite composition methods, PSCs have achieved remarkable efficiency improvements, reaching 23%. According to the latest data on the NREL PV chart, the most recent breakthrough has demonstrated a power conversion efficiency of 25.2%. The rapid increase in PCE from 3.8% to 25.2% within a decade positions perovskite solar cells as potential replacements for widely used silicon-based solar cells [10].

2.1.1 Basic Structure of Perovskite Solar Cells

Despite promising results in power conversion efficiency and cost-effective fabrication, PSCs face challenges such as the toxicity of lead and short-term stability. The typical structure of perovskite solar cells includes a perovskite absorber layer, an electron transport layer (ETL), and a hole transport layer (HTL). The ETL plays a critical role by extracting electrons from the perovskite layer and transporting them to the external circuit while preventing electron-hole recombination. Overcoming these challenges is essential for the continued development and commercialization of perovskite solar cells.

The active layer is the perovskite layer, which is where light is transformed to electrical power usually composed of the metal halide perovskite known as methylammonium lead iodide (MAPbI3). The perovskite is positioned above the hole transport layer (HTL). The holes are moved from the perovskite layer to the rear contact with the help of the HTL. For the HTL, materials like spiro-OMeTAD or PEDOT:PSS are frequently utilized. The rear contact, which functions as the topmost layer, is often an electrode made of gold or silver metal. It is collecting the electrons generated by the perovskite layer and facilitates their removal from the solar cell.

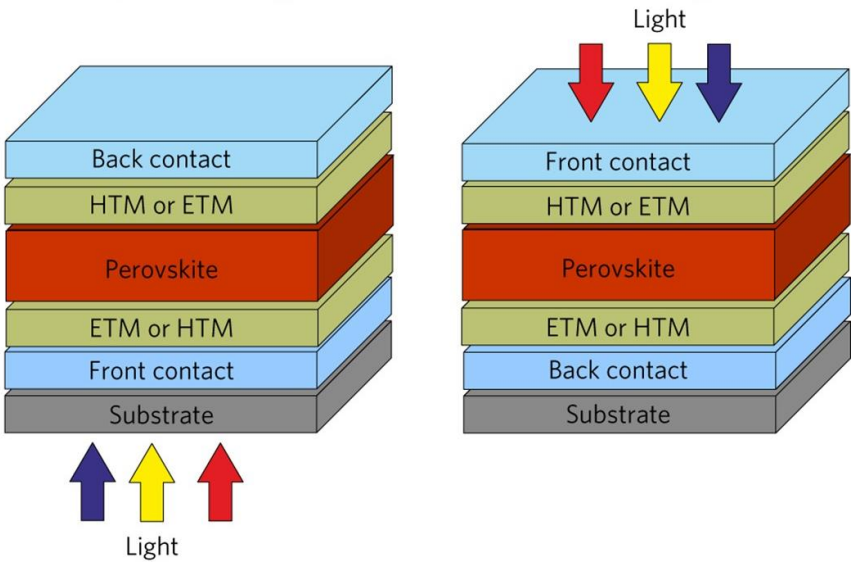

Figure 2.1: Basic structure of PSC

2.1.2 Advantage of Perovskite Solar Cells

Perovskite solar cells offer several advantages and benefits. They have demonstrated high efficiency in converting solar energy into electricity, surpassing many thin-film solar cell technologies and potentially matching or exceeding traditional silicon-based solar cells. Economically, perovskite solar cells can be manufactured at a low cost using cost-effective solution-based techniques such as spin-coating, inkjet printing, or spray deposition. This affordability opens up avenues for scalable and budget-friendly production, suitable for large-scale deployment.

Moreover, perovskite solar cells are versatile, capable of being produced on various substrates including flexible and lightweight materials like plastics. This adaptability allows integration into diverse applications such as curved surfaces, portable electronics, building-integrated photovoltaics (BIPV), and wearable devices. Their optical and electrical properties can be finely tuned by adjusting the chemical

composition of perovskite materials. This flexibility enables researchers to optimize the bandgap and optical characteristics, enhancing sunlight absorption and potentially achieving higher efficiencies.

The field of perovskite solar cell research has also seen rapid technological advancements. Continuous breakthroughs in materials, device architectures, and manufacturing techniques underscore its dynamic nature and promise ongoing improvements. These advancements pave the way for future commercialization and widespread adoption of perovskite solar cells in renewable energy applications.

2.2 Tin Halide Perovskite Cell

Generally, two major device architectures are documented for the PSCs which are planar heterojunction (n-i-p) and inverted structure (p-i-n) as shown in Figure 2.2. For planar heterojunction PSCs, the ETL is coated on a glass substrate that contains transparent conducting oxide (TCO), such as fluorine-doped tin oxide (FTO) or indium-doped tin oxide (ITO), using a variety of deposition techniques including spin coating, spray pyrolysis, chemical vapor deposition (CVD) etc. [11]

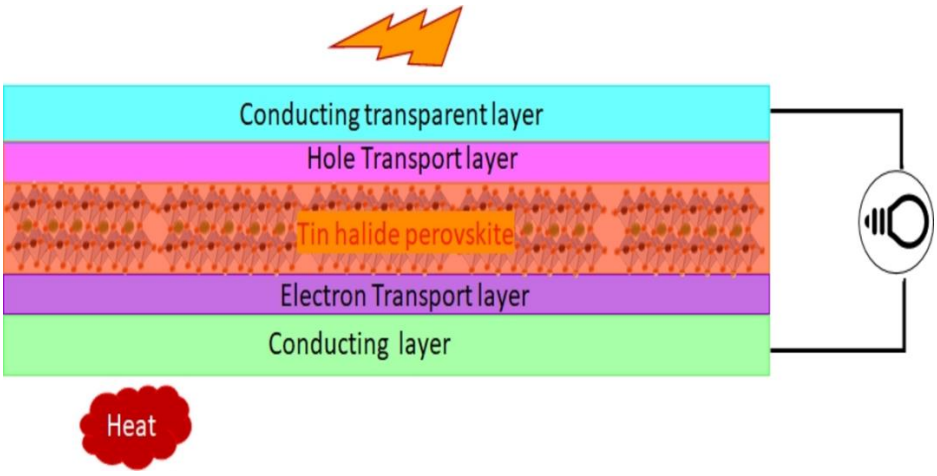

Figure 2.2: Basic Structure of Tin Halide Perovskite Solar Cells

Tin halide perovskites exhibit several intriguing material properties that make them a promising candidate for photovoltaic applications. These materials typically follow the formula ASnX3, where 'A' is a cation such as methylammonium (MA) or formamidine (FA), and 'X' is a halide such as iodine, bromine, or chlorine. Tin halide perovskites are known for their high absorption coefficients, which enable efficient light harvesting even with thin layers. They also possess suitable band gaps, which are crucial for achieving high power conversion efficiencies. Moreover, these materials exhibit good charge carrier mobilities and long carrier diffusion lengths, which are essential for efficient charge transport and reduced recombination losses. The combination of these properties contributes to the high potential of tin halide perovskites in solar cell applications.

One of the primary advantages of tin halide perovskites is their environmental friendliness compared to their lead-based counterparts. Tin is less toxic than lead, making tin halide perovskites a more sustainable choice for large-scale deployment. Additionally, the optoelectronic properties of tin halide perovskites, such as tenable band gaps and strong light absorption, make them highly suitable for efficient solar energy conversion. However, the development of tin halide perovskite solar cells also presents significant challenges. The most critical issue is the tendency of tin to oxidize from Sn2+ to Sn4+, which leads to instability in the perovskite structure and degradation of the solar cell's performance over time. This oxidation process results in increased defect densities and reduced charge carrier lifetimes, ultimately limiting the efficiency and longevity of the solar cells

In conclusion, while tin halide perovskite solar cells offer notable advantages in terms of environmental impact and promising material properties, overcoming the challenges associated with their stability and fabrication is crucial for their successful commercialization. Advances in material engineering, such as the incorporation of stabilizing additives and the development of more robust fabrication techniques, are essential to address these issues and unlock the full potential of tin halide perovskite solar cells in the renewable energy market.

2.3 SCAPS-1D Simulation Software

SCAPS-1D, developed at the Department of Electronics and Information Systems (ELIS) of the University of Gent in Ghent, Belgium, is a powerful one-dimensional simulation tool tailored for solar cells [5]. Designed to handle up to seven semiconductor layers, SCAPS-1D facilitates comprehensive simulation of multilayer solar cell structures [9]. It provides a range of electrical outputs crucial for solar cell analysis, including power conversion efficiency (PCE), hetero-junction energy band structures, current-voltage (J-V) characteristics, open circuit voltage (VOC), short circuit current (JSC), quantum efficiency (QE), current density, and fill factor (FF).

Key to its functionality are advanced algorithms that solve Poisson's equation and continuity equations for both charge carriers and holes, ensuring accurate device modeling [12]. SCAPS-1D supports various modeling aspects such as physical models, parameter extraction from experimental data, interface characterization between different layers, and sensitivity analysis of key parameters affecting device performance.

Researchers can define and simulate intricate device architectures, inputting details like material properties, layer thicknesses, doping concentrations, and more to replicate real-world solar cell behavior effectively. The software's capability to simulate carrier transport, recombination, optical absorption, and other critical phenomena enables detailed analysis and optimization of solar cell designs.

SCAPS-1D plays a vital role in photovoltaics research, particularly for exploring and improving diverse solar cell technologies, including perovskite solar cells. It helps identify performance limitations, enhance efficiency, and optimize solar cell designs, thereby contributing to the development of more efficient and reliable photovoltaic devices.

2.4 Taguchi Method

The Taguchi method serves as a strategy for enhancing the quality of analyzed processes and products. Operating on a predictive model, particularly in the analysis of Signal-to-Noise (S/N) ratios, this method allows the control of numerous components to restrict parameter changes and modify the experimental process under consistent circumstances. Consequently, this leads to an improved analysis of responses and physical attributes [13]. The Taguchi method has proven to be a reliable and reputable approach, demonstrating effectiveness across various systems and materials with high complexity in scientific, engineering, and industrial domains [13].

Employed as a technique to pinpoint crucial aspects in achieving favorable outcomes within manufacturing processes, the Taguchi method systematically alters these variables at two or more levels. Absike et. al., (2022) demonstrated that the Taguchi method was applied to the development and characterization of copper oxide

thin films, optimizing their structural and optical properties under optimal conditions. Three parameters, namely Cu2+ content, preheating temperature (TP), and final heat-treatment temperature, were selected [4].

The Signal-to-Noise ratio (S/N) was employed to scrutinize experimental data and identify elements influencing the response. In accordance with the Taguchi method, the best values for each chosen experiment were determined by comparing the Signal-to-Noise (S/N) ratio, aiming for a "the greater, the better" response and superior device performance [4].

2.4.1 Orthogonal Array

The Taguchi Orthogonal Array (OA) design represents a type of general fractional factorial design introduced by Dr. Genichi Taguchi. This design matrix is structured to efficiently explore a subset of combinations of different factors and their levels. It ensures each level of every factor is equally represented, maintaining balance across the experimental setup. This balanced nature allows for independent assessment of each element despite the complexity of interactions.

One of the significant advantages of using Orthogonal Arrays (OA) in experimental design is evident in the Taguchi method's optimization process. By employing OA, the Taguchi method significantly reduces the complexity of experimental planning, especially when dealing with numerous experimental runs. This streamlined approach helps minimize the number of experiments required to achieve optimization goals, thereby enhancing efficiency in the optimization process [14].

2.4.2 Experiment Design Strategy

The Taguchi technique utilizes a distinctive set of orthogonal arrays (OAs) to structure experimental trials. For instance, a sample OA designed for three-level factors accommodates up to four components with three levels each. This specific OA as shown in Table 2.1 consists of nine rows and four columns, where each row represents a different factor levels across experiments. The columns correspond to the listed factors in the study, with each column systematically comprising three conditions at levels 1, 2, and 3. This design, known as the L design, ensures orthogonality among the four columns, facilitating effective experimentation [15].

Table 2.1: Taguchi Method Experiment Design

Expt. No.	Control Factors			
	A	B	C	D
1	1	1	1	1
2	1	2	2	2
3	1	3	3	3
4	2	1	2	3
5	2	2	3	1
6	2	3	1	2
7	3	1	3	2
8	3	2	1	3
9	3	3	2	1

The orthogonal array (OA) greatly simplifies the experiment design process by guiding the selection of the most suitable array, assigning elements to appropriate columns, and outlining combinations for individual trial experiments. This standardization ensures consistency across experiments, as all possible combinations

are covered within the defined columns, regardless of how experimenters choose to allocate them. This approach, involving nine trial runs, promotes uniformity in experiment design [4].

In the context of this research, optimizing all parameters for Perovskite Solar Cells is crucial for achieving peak performance. Efficient optimization of manufacturing processes and product characteristics is key to enhancing performance and reducing production costs. The Taguchi method offers a systematic and efficient approach to experiment design, requiring minimal trials to achieve desired outcomes.

CHAPTER 3

METHODOLOGY

This segment elucidates the utilization of data and information obtained through a specific method to attain the project's goals. It encompasses a fundamental flowchart designed to enhance clarity and methodological precision, ensuring the accomplishment of superior outcomes. Within this section, an inclusive overview of the chosen technique will be presented, encompassing the entire scope of the project.

3.1 Overview

The analysis comprises two components: simulation and optimization of results using the Taguchi method. The simulation phase employs the SCAPS-1D software, initially modeling the solar structure of Tin Halide Perovskite Solar Cells to assess optimal efficiency. This investigation delves into various aspects of the Tin Halide PSC structure, encompassing factors like working temperature, material thickness,

defect density, and absorber material choice. SCAPS-1D generates I-V characteristics, enabling the evaluation of parameters such as Power Conversion Efficiency (PCE), Fill Factor (FF), Open-Circuit Voltage (Voc), and Short-Circuit Current (Jsc). Subsequently, the collected data undergoes optimization using the Taguchi method to yield more effective and refined results.

3.2 Flowchart of the project

Within this project, various methods have been implemented to achieve the intended outcomes. The detailed explanation of each step will be elucidated according to the presented flowchart as shown in Figure 3.1.

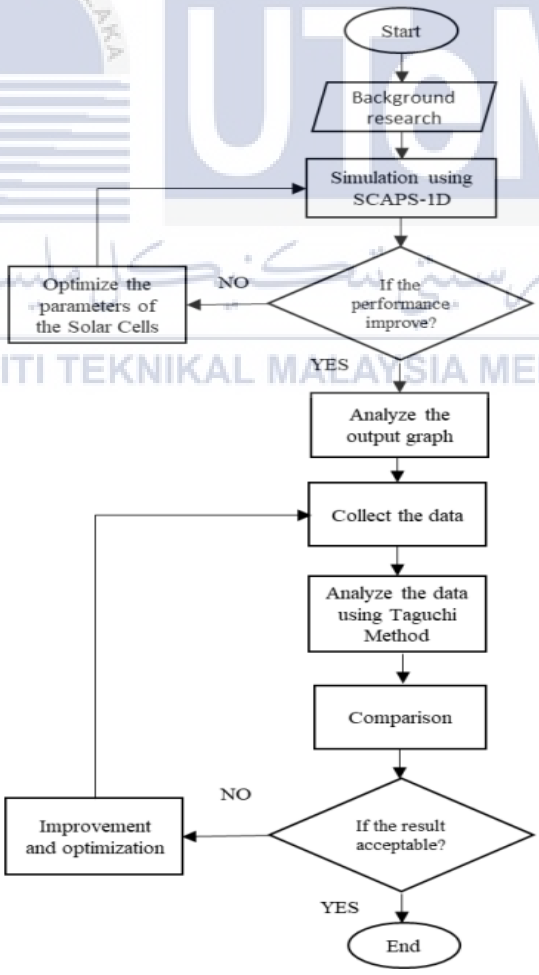

Figure 3.1: Flowchart of the Project

3.3 Numerical Method for Device Simulation

The simulation process involves several steps, starting with defining the problem and specifying essential parameters. Subsequently, the configuration of working conditions, including temperature and spectrum, is undertaken. The next step is to outline the desired output measurement, followed by the execution of the simulation. The sequence for initiating simulations with SCAPS-1D is straightforward yet comprehensive. SCAPS-1D serves as a valuable tool for assessing the impact of different materials on device performance, enabling researchers to simulate device behavior with varied material combinations and optimize their properties. Moreover, it aids in investigating the effects of diverse processing steps on device characteristics, contributing to more effective process optimization and efficiency enhancement.

3.3.1 Simulation using SCAPS-1D

SCAPS-1D, in its version 3.3.10, is a numerical modeling simulation tool designed for up to seven semiconductor layers. Developed by a photovoltaic researcher from the University of Gent's Department of Electronics and Information Systems, this tool is specifically tailored for solar cell devices with multiple semiconductor layers. SCAPS-1D is proficient in extracting crucial electrical parameters such as acceptor and donor density, current densities, and more. It achieves this by solving the Poisson Equation (3.1) and the continuity equations for electrons and holes are Equations (3.2) and (3.3) respectively. The programmed equations within SCAPS-1D contribute to providing comprehensive insights into the spectrum response of solar radiation and the current-voltage (J-V) characteristics of the solar cell [13].

$$\frac{d}{dx}[\varepsilon(x)\frac{d\Psi}{dx}] = q\,[p(x) - n(x) + N_D^+(x) - N_A^-(x) + p_t(x) - n_t(x)] \quad (3.1)$$

$$-\frac{1}{q}\frac{dJ_n}{dx} + R_n(x) - G(x) = 0 \quad (3.2)$$

$$\frac{1}{q}\frac{dJ_p}{dx} + R_p(x) - G(x) = 0 \quad (3.3)$$

Where, Ψ = electrostatic potential, ε = dielectric permittivity (relative), x = denotes the position, **NA** − = ionized acceptor, **ND** + = ionized donor, p = holes, e = electrons, **pt** = number of trapped holes, **nt** = number of trapped electrons, **Jp** = holes current density, **Jn** = electrons current density, G(x) = generation rates, **Rp** (x) = recombination rate of holes and **Rn** (x) = recombination rate of electrons. It allows the user to model the bandgap energy diagram and the I-V curve of a solar cell by constructing a p-n junction, adding contacts, and simulating the bandgap energy diagram and I-V curve. SCAPS is a simple application that may be used for both research and education.

3.3.2 Problem Setting in SCAPS-1D

Within SCAPS-1D, the problem-setting function is employed to formulate the structure of each layer in the solar cell, incorporating electrical parameters and establishing interfaces between layers. The action-setting feature is utilized to specify the solar cell configuration for simulation, encompassing adjustments such as I-V quality scale, C-V capacitance voltage, C-f capacitance frequency, and QE quantum efficiency. For this specific experiment, solely the I-V configuration is utilized to ascertain the power conversion efficiency (PCE). The voltage range of the solar cell, delimited between V1 and V2, is fixed at 0 V and 2 V, respectively. The illumination setting is instrumental in defining both the range and direction of prevailing light conditions, whether dim or bright. Standardizing the illumination, the brightness is set

to AM1.5G, 100 mWcm², and the light is activated within the illumination setting. Prior to initiating calculations, the temperature of the solar intensity must be established. For this research, the temperature is consistently set at 300K in Kelvin units.

Figure 3.2 shows the SCAPS-1D software and it consists of four settings. After clicking on set problem, as shown in Figure 3.3, the solar cell defining board is opened. There are three classifications on this board. There are five options on it. These options have the ability to create new design, load previous design and save construction records in the SCAPS definition library. The layers of the solar cell are saved as '.def' files. After characterizing the design, the 'OK' button is clicked.

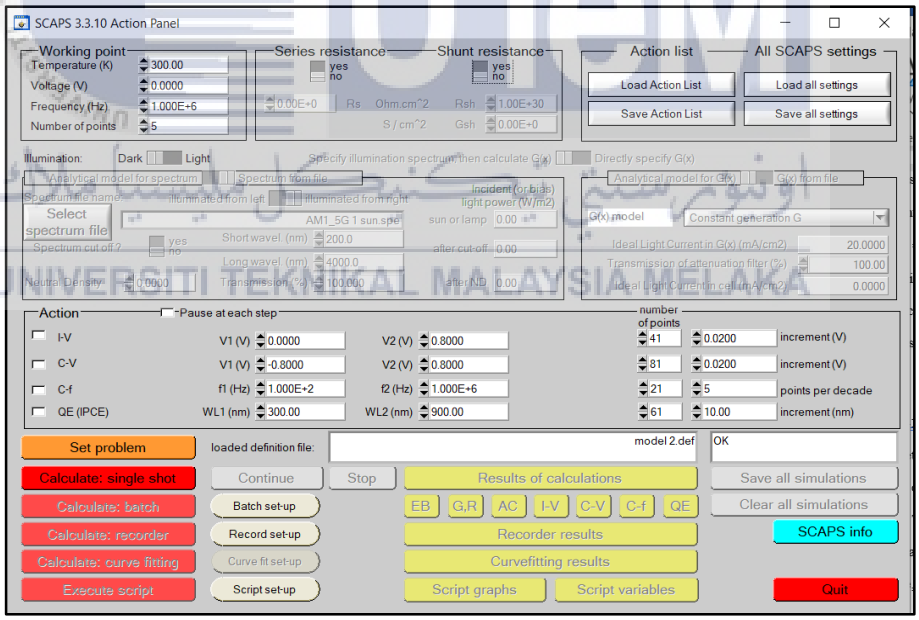

Figure 3.2: SCAPS-1D Action Panel

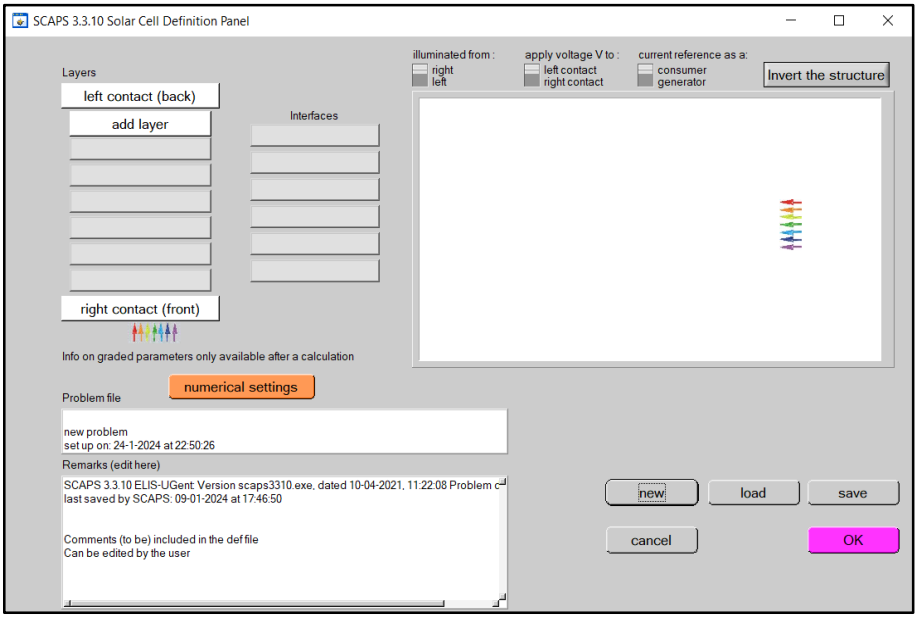

Figure 3.3: SCAPS-1D Material Configuration

3.3.3 Adding Layer to Structure in SCAPS-1D

As depicted in Figure 3.4, the setting layer encompasses interfaces between layers, back and front contacts, and mathematical inclinations. SCAPS-1D is specifically designed to facilitate the construction of a solar cell with a maximum of seven layers. Within this module, the orientation of illumination can be altered, either from the left or right. Various options are available for applied voltage and current, providing flexibility in experimentation. The thickness and color of each layer in the solar cell can be visualized, as illustrated in Figure 3.4. The Layer Properties panel in SCAPS-1D serves as a platform for inputting the electrical parameters corresponding to each material layer. The mathematical boundaries for each layer in PSC devices are established based on input parameters from prior research, as detailed in Table 3.1.

Table 3.1: SCAPS-1D Input Parameter of Numerical for each Layer in Tin Halide PSC Devices [2].

Material Properties	CuI	$CH_3NH_3SnI_3$	CH_3NH_3SnBr	TiO_2	ZnO:Al
Thickness, d (um)	0.2	0.7	0.3	0.1	0.2
Band gap (eV)	3.1	1.3	2.15	3.26	3.3
Electron affinity (eV)	2.1	4.17	4.17	4.2	4.6
Dielectric permittivity	6.5	6.5	10.0	10.0	9.0
CB effective density of states ($1/cm^3$)	2.2E +19	1.0E+18	2.5E+19	2.2E+18	2.2E+18
VB effective density of states ($1/cm^3$)	1.8E+19	1.0E+19	2.5E+19	1.8E+19	1.8E+19
Electron thermal velocity	1.1E+7	1.0E+6	1.0E+7	1.0E+7	1.0E+7
Hole thermal velocity (cm/s)	1.1E+7	1.0E+6	1.0E+7	1.0E+7	1.0E+7
Electron mobility (cm^2/vs)	1.0E+2	1.6E+0	1.6E+0	1.0E+2	1.0E+2
Hole mobility (cm^2/vs)	4.39E+1	1.6E+0	1.6E+0	2.5E+1	2.5E+1
Shallow uniform donor density Nd	0	1.0E+19	0	1.0E+19	1.0E+18
Shallow uniform acceptor density Na	1.0E+18	3.2E+15	3.2E+15	0	0

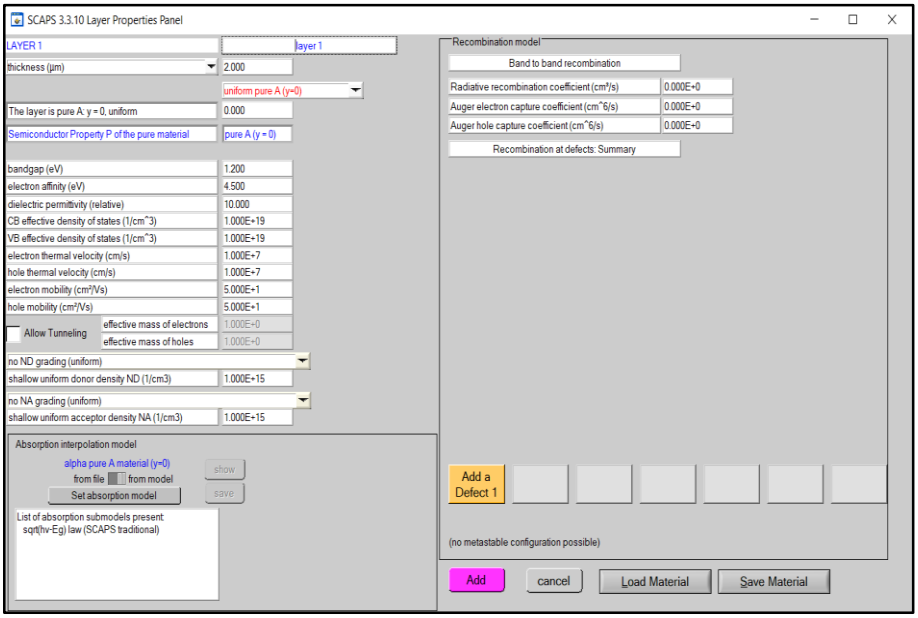

Figure 3.4: SCAPS-1D Electrical Parameter

3.3.4 SCAPS-1D Simulation for Tin Halide PSC Device

In this experiment, three architectures for Tin Halide Perovskite Solar Cells (PSCs) were evaluated. The first architecture consists of tin perovskite solar cells without a hole transport material (HTM), exhibiting high stability, straightforward fabrication, and cost-effectiveness. Notably, in these devices, the absorber material serves dual roles, functioning both as an HTM and a light absorber, specifically in the configuration of Glass/ZnO:Al/TiO2/CH3NH3SnI3/Au. The second architecture, as shown in Figure 3.5, features a planar junction with the structure Glass/ZnO:Al/TiO2/CH3NH3SnI3/CuI/Au. The third architecture includes a dual layer of absorber materials, with the configuration Glass/ZnO:Al/TiO2/CH3NH3SnBr3/CH3NH3SnI3/CuI/Au. For this project, the architecture with the highest Power Conversion Efficiency (PCE) was chosen for optimization, with model A being the selected one.

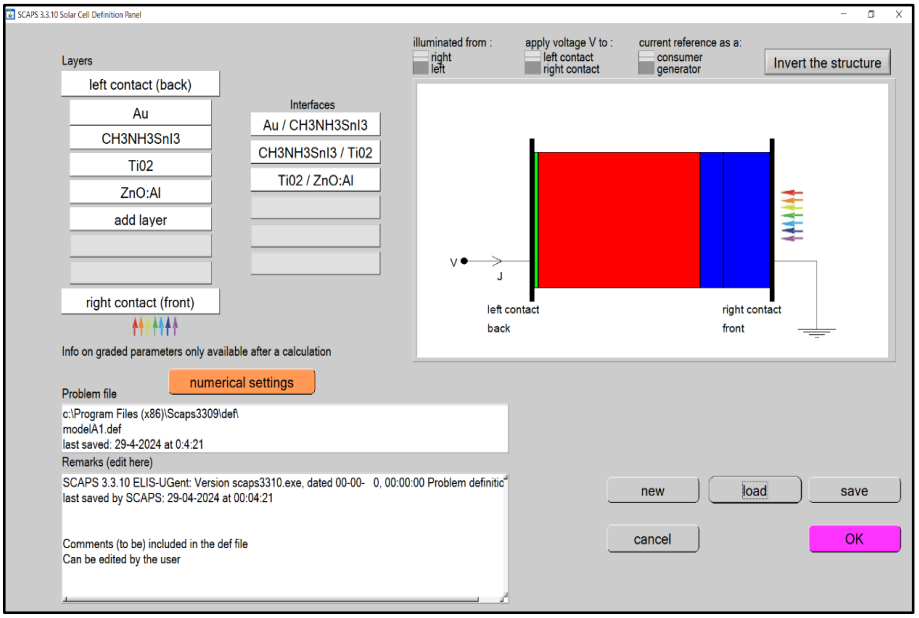

Figure 3.5: Structure model A

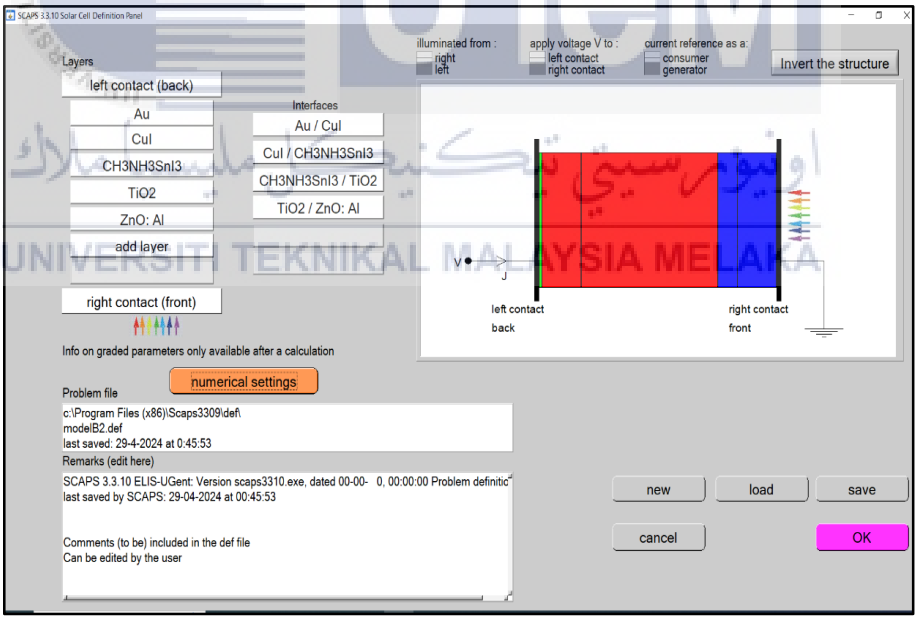

Figure 3.6: Structure model B

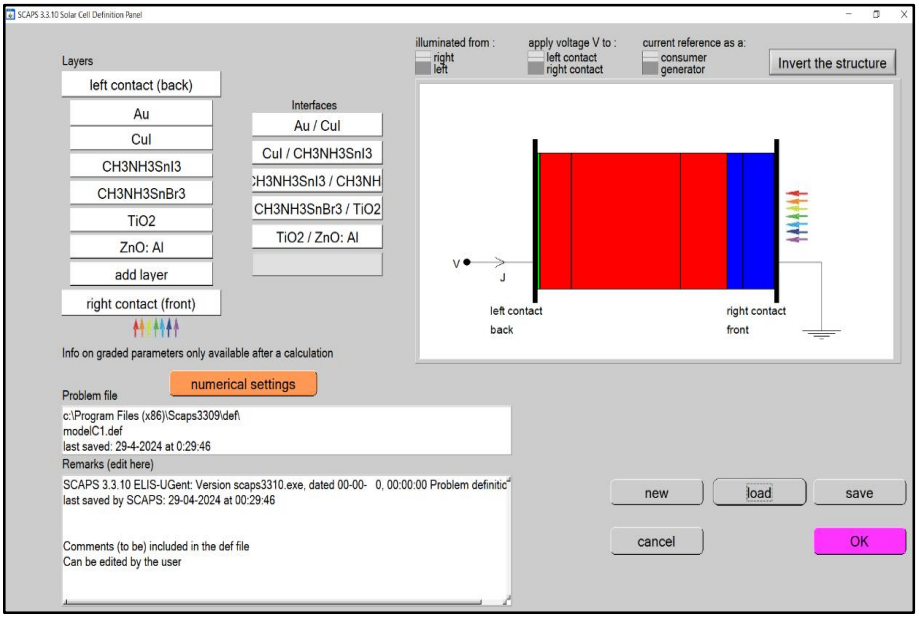

Figure 3.7: Structure model C

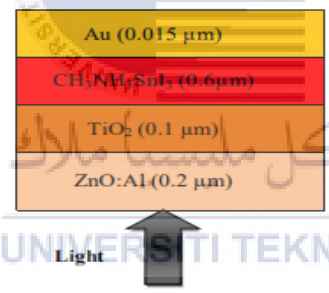

Figure 3.8: 1st architecture

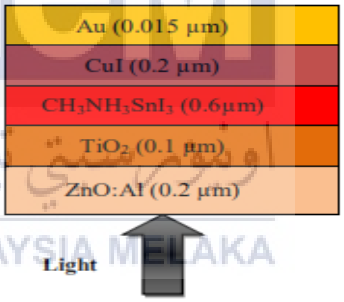

Figure 3.9: 2nd architecture

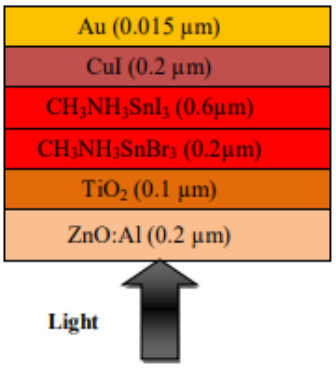

Figure 3.10: 3rd architecture

Finally, after simulation, the I-V curve will be analyzed and see the performance of IPSC through PCE. From I-V curve it shows the Voc, Jsc, FF and PCE. In any case, if the results do not match the ideal result, the method should be reviewed until the ideal result is achieved.

3.4 Taguchi Method for Optimization Approach

The primary implementation processes for optimizing input process parameters using the Taguchi method are illustrated in Figure 3.11. The Taguchi method was employed in this project to ascertain the optimal solution for Tin Halide PSC devices.

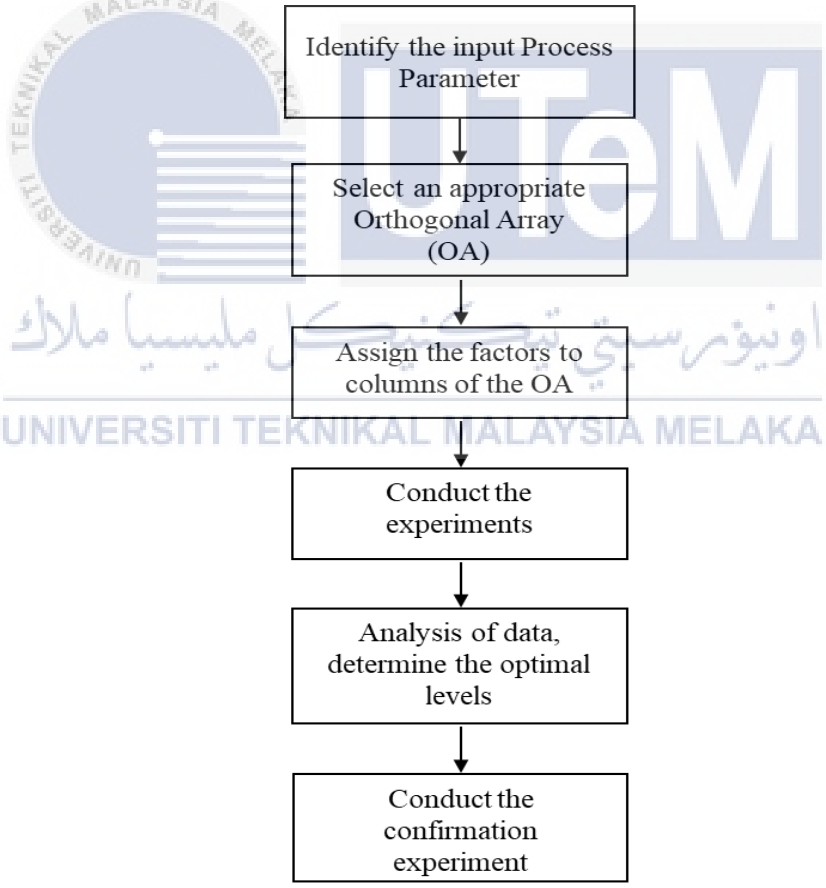

Figure 3.11: Flowchart of Taguchi Method

This method underscores the importance of designing and conducting experiments to gauge the influence of input process parameters on output responses. Through the analysis of various components, it becomes possible to pinpoint the optimal combination of factors.

3.4.1 Identification of Process Parameters

The main electrical parameters or control factors that were selected to analyzed the most impact of process parameters on the predictive modelling characteristics are displayed in Table 3.2. This table illustrates the symbols represented as A, B, C and D as the respective electrical parameters.

Table 3-2: Electrical Parameters Selected

Symbol	Electrical Parameter	Units
A	Perovskite Thickness	µm
B	Tio2 Thickness	µm
C	Perovskite Donor Density	cm^{-3}
D	Tio2 Donor Density	cm^{-3}

3.4.2 Selection of Orthogonal Array

Orthogonal array (OA) can reduce the number of experimental. In order to choose an appropriate orthogonal array (OA) it depends on the total of parameter. In these experiments, L9 OA was used. It has 9 experiments with 4 control factors. Taguchi L9 OA greatly can reduce the number of tests and increase the efficiency. The experimental layout for the process parameters employing an orthogonal array of L9. The L9 orthogonal array is used to comprehend the effect of four control factors whose levels were altered throughout nine rows of experiments.

Table 3.3: L9 orthogonal array Taguchi

Expt. No.	Control Factors				S/N Ratio (dB)
	A	B	C	D	
1	1	1	1	1	η1
2	1	2	2	2	η2
3	1	3	3	3	η3
4	2	1	2	3	η4
5	2	2	3	1	η5
6	2	3	1	2	η6
7	3	1	3	2	η7
8	3	2	1	3	η8
9	3	3	2	1	η9

3.4.3 Analysis of Variance (ANOVA)

The Taguchi Method is included in the analysis to identify which factors have the greatest impact on improving results and to determine the optimum values for these factors. The purpose of the Analysis of Variance (ANOVA) is to quantify the percentage contribution of each process parameter to the experimental results. ANOVA calculates parameters such as Sum of Squares (SSQ), Degree of Freedom (DF), variance, F-value, and the percentage contribution of each factor. The Sum of Squares measures the deviation of the experimental data from the mean value. The total sum of squares (SSQ_T) can be calculated as given in the following (15);

$$\mathrm{SSQ_T} = \sum_{i=1}^{n}(\eta_i - m)^2 \tag{3.4}$$

Where,

$$m = \frac{1}{n}\left[\sum_{i=1}^{n}(\eta_i)\right] \tag{3.5}$$

Where η is the number of experiments in the orthogonal array, ηi is the mean of the S/N ratio for the ith experiment, and m is the average of all η_i values. By examining column one until four of the orthogonal arrays in Table 3.3, observe that all three levels of every factor are equally represented in the nine experiments. Thus, m is a balanced overall mean over the entire experiment region, whereas the SSQ_p is the sum of square of average performance of a factor at each level (15);

$$\mathrm{SSQ_{p(X)}} = \mathrm{k}\left[\sum_{\mathrm{j=1}}^{\mathrm{k}}(\mathrm{m_{Xj}} - \mathrm{m})^2\right] \tag{3.6}$$

Where X is the symbol of process parameters, k is the number of levels for the factor, j is the level of factor, and m_{Xj} is the effect of a factor level. m_{Xj} refers to the deviation from the overall mean. The degree of freedom (DF) of the tested process parameter, where t is the repetition of each level of the process parameters.

$$\mathrm{DF} = \mathrm{t} - 1 \tag{3.7}$$

DF, rather than the number of observations, had been used in the variance calculation. The variance (mean square) of the process parameter tested, V_p is given as;

$$\mathrm{V_p} = \frac{\mathrm{SSQ_p}}{\mathrm{DF}} \tag{3.8}$$

F-value for each process parameter is the ratio of variance due to the effect of a factor and variance due to the error term, V_e;

$$\mathrm{F_p} = \frac{\mathrm{V_p}}{\mathrm{V_e}} \tag{3.9}$$

F-value is used to measure the significance of the factor under investigation with respect to the variance of all the factors, including error term. Usually, the larger the F-value, the greater the effect of performance characteristic due to the change of process parameter [4]. The percentage contribution for each factor is the ratio of the factor sum to the total expressed in percentage. For instance, the percentage contribution (ρ) due to Factor A, ρ_A can be calculated as;

$$\rho_A = \frac{SSQ_{p(A)}}{SS_T} x100 \tag{3.10}$$

When the variance of the error is equal to zero, the F-value, F_p for the factors is undetermined. Then, the variance of the error can be combined with another smallest factor variance in order to calculate a new error variance, which can be used to produce meaningful results. The process of disregarding and the contribution of individual factor subsequently adjusted the contribution of the other factor known as pooling.

3.4.4 Larger is Better

The target is to maximize the respond. The bigger the S/N, the better it is calculated to be. Since our aim is to maximize strength, the compressive strength in the current study should be higher. Equation (3.11) shows the Ƞ for the quality characteristics of higher-the-better. The number of tests and experimental value of the obtained respond characteristics being represented as n and Yn respectively [15].

$$\eta = -10 \log_{10} \left[\frac{1}{n} \sum \left(\frac{1}{Y1^2} + \frac{1}{Y2^2} + \cdots + \frac{1}{Y3^3}\right)\right] \tag{3.11}$$

Experimentation can be utilized, for instance, to examine the influence of Factor A at level 3 (A3). Level A3 of factor A was observed in experiments 7, 8, and 9. The

average S/N ratio for these experiments, denoted by, m$A3$ is calculated as follows [15]:

$$m_{A_3} = \frac{1}{3}[\eta_7 + \eta_8 + \eta_9] \quad (3.12)$$

Thus, the effect of Factor A at level A3 is given by ($m_{A3} - m$) from Table 3.3; for experiments 7, 8, and 9, the level of Factor B is 1, 2, and 3, respectively. Similarly, the levels of Factors C and D had the values 1, 2, and 3 for these experiments. Therefore, the amount m_{A3} reflects an average when the thickness of GO is at level A3, where the averaging is performed in a balanced fashion across all levels of the other three components.

$$m_{B_2} = \frac{1}{3}[\eta_2 + \eta_5 + \eta_8] \quad (3.13)$$

The average S/N ratio for levels A1 and A2 of Factor A, as well as the ratios for the various levels of the other components, can be calculated in the same manner. The average S/N ratio at level B2 for Factor B. Since the matrix experiment is built on an orthogonal array, all level averages share the same balancing property as m_{A3}.

3.4.5 Confirmation Experiment

In this experiment, initially, 5 control factors were selected, and an L8 orthogonal array was employed, comprising 8 experiments with these 5 control factors. However, the subsequent analysis revealed that only 4 control factors exhibited higher significance in terms of Signal-to-Noise (S/N) ratio compared to the consistently pooled or neutral temperature across all process parameters. Consequently, an L9 orthogonal array with 9 experiments and 4 control factors was chosen for further investigation.

The concluding step in the design of the experiment process involves a confirmation experiment. The primary objective of this confirmation experiment is to validate the conclusions drawn during the analysis phase [4]. After determining the optimal levels of process parameters, a confirmation test or final simulation is conducted to verify the accuracy of the predictions made by the Taguchi Method. The necessity for a confirmatory test arises if the optimal combination of parameters and their levels aligns with one of the experiments in the orthogonal array. Utilizing specific equations, the estimated value of the response characteristic under optimal conditions can be computed by adding the average performance to the contribution of each parameter at its optimal level [15].

$$Y_{opt} = m + \sum_{i=1}^{n} (m_{iopt} - m) \quad (3.14)$$

Where m represents the average performance, n represents the number of process parameters or control variables, and m iopt represents the average process parameter at the optimal level.

CHAPTER 4

RESULT AND DISCUSSION

In this chapter will discuss regarding the outcome that has been successfully obtained from the simulation process in this project. Different parameter has been analyzed using Taguchi method L9 (OA) and the results will be discussed to obtain a better performance of the device. Then, all the parameters will be related with theory and discussed regarding problem faces during an experiment.

4.1 Introduction to Taguchi Method Analysis

The Taguchi method, developed by Genichi Taguchi, is a statistical approach used to improve the quality of products or processes by reducing variation and enhancing performance. This method involves defining control factors (things you can change), noise factors (things you can't control), and response variables (results you measure). By using specially designed experiments called orthogonal arrays, the Taguchi method efficiently tests different combinations of these factors, ensuring all possibilities are covered with fewer experiments.

Instead of just using traditional statistics like mean and standard deviation, the Taguchi method uses the Signal-to-Noise (S/N) ratio. This ratio compares the desired outcome (signal) to the undesired variation (noise). The higher the S/N ratio, the better the performance.

Overall, the Taguchi method provides a structured and efficient way to optimize products or processes, considering variations and factors that might affect quality. It helps identify the best settings to reduce variation and improve overall quality.

4.2 Analysis Tin Halide Perovskite using SCAPS- 1D

Three different models for tin halide perovskite solar cells were designed and simulated using SCAPS-1D software. The goal was to evaluate the performance of each model and select the one with the highest Power Conversion Efficiency (PCE) for further optimization using the Taguchi method. The PCE values obtained for the three models are summarized in Table 4.1.

Table 4.1: Comparison result using simulation SCAPS-1D

Material	Output							
	Jsc (mA/cm^2)		Voc (V)		FF (%)		PCE (%)	
	Past paper [2]	Simulate	Past paper [2]	Simulate	Past paper [2]	Simulate	Past paper [2]	Simulate
Glass/ZnO:Al/TiO2/ CH3NH3SnI3/Au **(Model A)**	18.15	21.23	0.95	0.96	84.05	84.22	25.26	26.24
Glass/ZnO:Al/TiO2/ CH3NH3SnI3/ CuI/Au **(Model B)**	31.84	33.77	0.95	0.96	50.99	51.01	15.55	16.52
Glass/ZnO:Al/TiO2/ CH3NH3SnBr3/ CH3NH3SnI3/ CuI/Au **(Model C)**	31.96	33.76	0.96	1.13	49.98	50.81	16.15	16.45

From the Table 4.1, it is evident that Model A exhibits a significantly higher PCE value of 26.24% compared to Model B and Model C, which have PCE values of 16.52% and 16.45%, respectively. This notable difference indicates that Model A is more efficient in converting solar energy into electrical energy. The superior performance of Model A can be attributed to the optimized layer thicknesses, material properties, and interface characteristics designed during the simulation process. In contrast, Models B and C, while still effective, did not achieve the same level of efficiency due to suboptimal parameter configurations.

To further validate the performance of Model A, we compared its PCE with those reported in previous studies. According to previous paper [2], the highest reported PCE for tin halide perovskite solar cells was approximately 25.26%. The PCE of 26.24% achieved by Model A not only surpasses this benchmark but also highlights the potential of our design approach in advancing the efficiency of perovskite solar cells. Given its superior performance, Model A was selected for further optimization using the Taguchi method. This method provides a systematic approach to identify the optimal conditions for the factors affecting the solar cell performance, thus further enhancing the PCE.

The Figure 4.1 illustrates the relationship between open-circuit voltage (Voc) and power conversion efficiency (PCE) for selected model A, experimental data, the current study's simulation results (my work), and a previous study's results (paper). Experimental data shows the lowest Voc value across the PCE range is 0.95 V, while results from the previous studies show a moderate Voc value of 0.96 V.

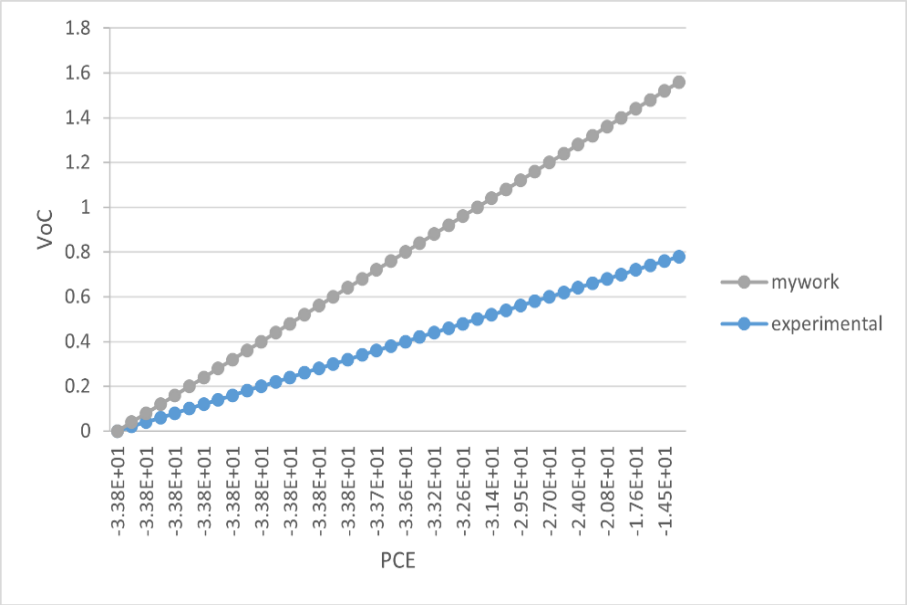

Figure 4.1: Graph comparison model A

In contrast, the current study's simulations demonstrate the highest Voc values, indicating superior performance. This positive correlation between Voc and PCE across all datasets highlights the advancements achieved in the current study. The optimized design and methodologies have significantly enhanced the solar cell's performance, surpassing both experimental results and previous studies. This improvement underscores the effectiveness of the new approaches employed in this research.

4.3 Analysis of Different Thickness of Perovskite in PSC.

Analyzed the thickness of Perovskite layer in order the improved the performance of Tin Halide PSC. Initially, the thickness of Perovskite varied from 0.1 um to 1.0 um. Table 4.2 shows the trend of varied thickness of Perovskite layer and each PCE value. Based on Table 4.2. it can be observed that as the thickness of Perovskite was varied

from 0.1 um to 1.0 um, the power conversion efficiency of Tin Halide decreases from 17.40% to 12.68 %.

Table 4.2 : The Range of Thickness of Perovskite

Perovskite thickness (um)	PCE (%)
0.1	15.07
0.2	15.20
0.3	16.80
0.4	16.30
0.5	17.10
0.6	17.40
0.7	17.40
0.8	15.51
0.9	15.07
1.0	12.68

4.4 Optimizing using Taguchi Method

The output parameters were analyzed using the Taguchi method with an L9 orthogonal array (OA), which consists of nine different experimental combinations. Table 4 shows the design of experiments using the L9 OA for the four output parameters: power conversion efficiency (PCE), fill factor (FF), open circuit voltage (Voc), and short circuit current (Jsc).

The experiments were conducted based on these orthogonal array designs, testing various combinations of control factor levels. The control factors, labeled as A, B, C, and D, represent buffer thickness, buffer donor density, perovskite thickness, and perovskite donor density, respectively. Each control factor has three different levels, as variations in these parameters can significantly impact the performance of the PSC device. Table 4.3 shows the experimental layout using L9 (3^4) orthogonal array.

The signal-to-noise (S/N) ratio was calculated to assess the impact of these factors on the outputs and interpret the findings of the study. Following the larger-the-better principle, the optimal values for each experimental run were determined by comparing the S/N ratios. Therefore, improvements in output parameters can be achieved by selecting appropriate testing conditions (settings of noise factors) during robust experimental designs. Table 4.4 and Table 4.5 illustrate the values of control factors and noise factors, respectively, along with their corresponding levels. Meanwhile, Table 4.5 shows two noise factors such as Au thickness and TiO2 acceptor density were incorporated into the experimental design. Each of these noise factors was varied across two levels to obtain values for PCE, FF, Voc, and Jsc.

Table 4.3: L9 Orthogonal Array Design of Experiments

Expt. No.	Control Factors				S/N Ratio (dB)
	A Perovskite Thickness	B TiO2 Thickness	C Perovskite Donor Density	D TiO2 Donor Density	
1	1	1	1	1	η1
2	1	2	2	2	η2
3	1	3	3	3	η3
4	2	1	2	3	η4
5	2	2	3	1	η5
6	2	3	1	2	η6
7	3	1	3	2	η7
8	3	2	1	3	η8
9	3	3	2	1	η9

Nine different experimental combinations were conducted using an orthogonal array table, incorporating varying levels of control and noise factors. Each set of parameter combinations was simulated in four experiments. The next step involves

determining which control factor has the most significant impact on the characteristics of the PSC device, based on the feedback obtained from PCE using the L9 orthogonal array.

Table 4.4: Control Factors and The Levels

Control Factor	Level		
	1	2	3
Perovskite Thickness (um) (A)	0.600	0.800	0.700
TiO2 Thickness (um) (B)	0.100	0.200	0.300
Perovskite Donor Density (cm^{-3}) (C)	$1x10^{17}$	$1 x 10^{18}$	$1 x 10^{19}$
Donor Density (cm^{-3}) (D)	$1 x 10^{19}$	$1 x 10^{18}$	$1x10^{17}$

Table 4.5: Noise Factors and The Level

Noise Factor	Level	
	1	2
Au Thickness (um) (N)	0.015	0.020
TiO2 Acceptor Density (um) (M)	$1x10^{17}$	$1 x 10^{18}$

The signal-to-noise (S/N) ratio facilitates the rapid identification of the most effective combinations. In this research, the PCE serves as a critical "larger-the-better" output parameter under observation. The prediction of PCE values following the use of the L9 array relies on this S/N ratio as a benchmark.

4.4.1 Optimization of PCE in Tin Halide Perovskite Solar Cell

Table 4.6 presents the PCE outcomes obtained from the PSC device using the L9 orthogonal array. The subsequent step involves establishing crucial values for

parameters such as buffer thickness, buffer donor density, perovskite thickness, and perovskite donor density, all of which may influence the output parameters. Meanwhile, Table 4.7 shows the signal-to-noise (S/N) ratios derived from the PCE experimental runs, adhering to the larger-the-better principle. Equation (3.11) was utilized to calculate η for each experiment.

Table 4.6: PCE Repetition Experiment Values

Exp No	Measurements for Each Experiment			
	1	2	3	4
1	15.07	15.07	14.87	14.87
2	1.68	1.68	1.69	1.69
3	1.52	1.52	1.32	1.32
4	1.63	1.63	1.63	1.63
5	1.71	1.71	1.72	1.72
6	15.51	15.51	15.3	15.3
7	1.74	1.74	1.74	1.74
8	12.68	12.68	12.48	12.48
9	1.74	1.74	1.74	1.74

The experimental design utilizing the orthogonal array allows for classification of the effect of each process parameter on the S/N ratio across different levels. Table 4.8 provides a summary of the S/N ratios corresponding to each level of control factors (CF). Table 4.8 also presents the ANOVA results for the power conversion efficiency (PCE) of the mixed halide PSC device. Generally, higher values of the signal-to-noise (S/N) ratio indicate better quality characteristics in PCE. Closer proximity to the target value signifies higher design quality [15].

Table 4.7: S/N Response for PCE

Mean Sum of Squares of reciprocals	SN Ratio (Larger-the-Better)
4.46E-03	23.50
3.52E-01	4.53
5.03E-01	2.98
3.76E-01	4.24
3.40E-01	4.69
4.21E-03	23.75
3.30E-01	4.81
6.32E-03	21.99
3.30E-01	4.81

Table 4.8: ANOVA Table for PCE

Control Factors	Level (dB)			DF	SSQ	MSQ	Factor effect (%)	empty or pooled F=<1.5
	1	2	3					
Perovskite Thickness	10.34	10.89	10.54	2	0	0	0	pooled
TiO2 thickness	10.85	10.40	10.51	2	0	0	0	pooled
Perovskite Donor Density	23.08	4.53	4.16	2	70.3	351	99	no
TiO2 Donor Density	11.00	11.03	9.74	2	3	2	0	pooled

For PCE, control factors such as buffer TiO2 Thickness (Factor B), perovskite donor density (Factor C), and TiO2 donor density (Factor D) at level 3 were identified as dominant factors due to their maximum S/N ratios (η). Specifically, Factor C (perovskite donor density) had the most significant effect on PCE, with a factor effect

of 99%. In contrast, Factors A, B, and D showed a 0% effect on PCE, indicating minimal influence on the PSC device's PCE.

Based on the S/N ratio analysis, the optimized levels for achieving high PCE were identified as A1B3C3D3. Figure 4.2 depicts the Larger-the-Better S/N Ratio graphs, where dotted lines represent the total mean of the S/N ratio values, and diamond plots denote the factor effects. This graphical representation, derived from Table 4.7, illustrates that higher levels of control factors correlate with higher dominance in achieving maximum S/N ratios (η).

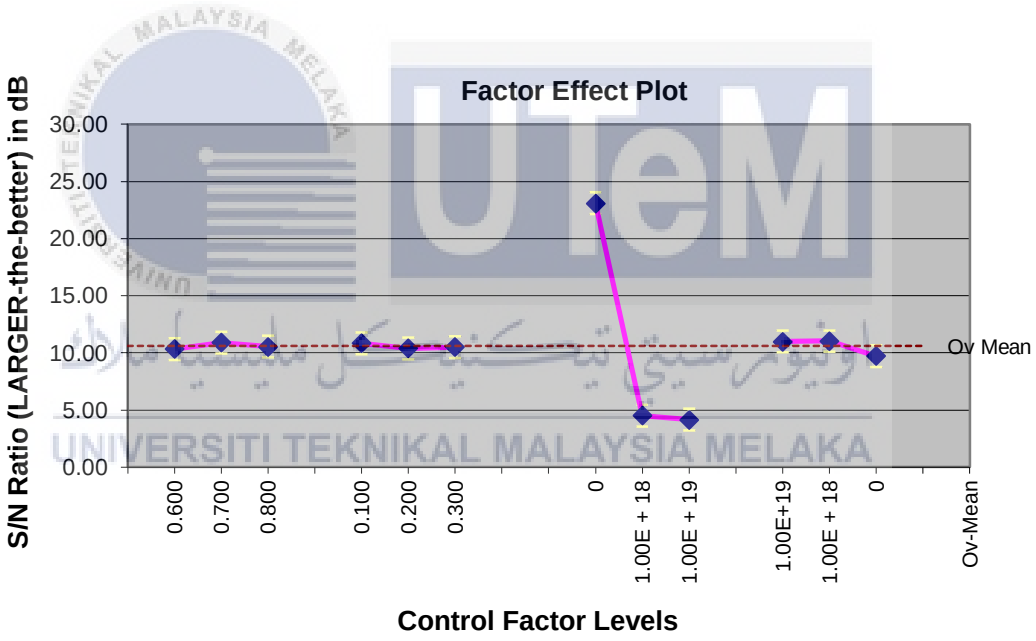

Figure 4.2: S/N Plot for PCE

Table 4.9 indicates the selection of levels based on their higher S/N ratios. Following the selection of optimal process parameters, the final step involves predicting and validating the enhancement of performance characteristics using these optimal levels. The S/N ratio at the optimal level of process parameters is recorded as

23.1 dB, falling within the anticipated range (24.41 dB to 21.76 dB). This prediction indicates improved performance characteristics based on the selected parameters.

Table 4.9: S/N Ratio Prediction for PCE

Control Factors	Level			Optimum Level	Factor effect (%)	Dominant, Significant or Neutral
	1	2	3			
Perovskite Thickness	0.600	0.800	0.700	2	0	Neutral
TiO2 Thickness	0.100	0.200	0.300	1	0	Neutral
Perovskite Donor Density	1E+17	1E+18	1E+19	1	99	Dominant
TiO2 Donor Density	1E+19	1E+18	1E+17	2	0	Neutral
S/N Ratio			23.1 dB			
	24.41 dB				21.76 dB	

4.4.2 Optimization of FF in Tin Halide Perovskite Solar Cell

The results for the fill factor (FF) in the PSC device using the L9 orthogonal array are presented in Table 4.10. Following the completion of all nine experiments within the L9 orthogonal array, the S/N ratio values were calculated using Equation (3.11), as detailed in Table 4.11. This table illustrates the S/N ratio values for the quality characteristics based on the Larger-the-Better principle after conducting nine experimental runs.

Table 4.12 provides a summary of the S/N ratios corresponding to each level of the process parameters. Additionally, it presents the overall mean S/N ratio calculated from the nine studies. For the fill factor (FF) of the PSC device, perovskite donor density (Factor C) and TiO2 donor density (Factor D) were identified as the primary

factors influencing FF, with percentages of 94% and 5%, respectively. These factors exhibit significant effects on the S/N ratio compared to other control factors. perovskite thickness (Factor A) has a lower effect percentage at 1%, while TiO2 thickness (Factor B) does not impact the fill factor, FF.

Table 4.10: FF Repetition Experiment Values

Exp No	Measurements for Each Experiment			
	1	2	3	4
1	7.73E+01	7.73E+01	7.73E+01	7.73E+01
2	4.88E+01	4.88E+01	4.88E+01	4.88E+01
3	4.46E+01	4.46E+01	4.46E+01	4.46E+01
4	4.63E+01	4.63E+01	4.63E+01	4.63E+01
5	4.91E+01	4.91E+01	4.91E+01	4.91E+01
6	7.77E+01	7.77E+01	7.77E+01	7.77E+01
7	4.91E+01	4.91E+01	4.41E+01	4.41E+01
8	6.57E+01	6.57E+01	6.56E+01	6.56E+01
9	4.90E+01	4.90E+01	4.90E+01	4.90E+01

Table 4.11: S/N Response FF

Mean Sum of Squares of reciprocals	SN Ratio (Larger-the-Better)
1.67E-04	37.77
4.20E-04	33.76
5.02E-04	32.99
4.66E-04	33.31
4.14E-04	33.83
1.66E-04	37.81
4.64E-04	33.33
2.32E-04	36.34
4.17E-04	33.80

Based on the analysis of average performance, the optimal condition is determined to be A2B3C1D1. This optimized combination is selected based on the plot depicted in Figure 4.3, which also aligns with the Larger-the-Better S/N ratio values shown in Table 4.12. Figure 4.3 illustrates the Larger-the-Better S/N Ratio graphs, where each control factor with a higher S/N Ratio (η) is considered dominant. Dotted lines represent the total mean of the S/N ratio values, while diamond plots indicate the effects of each factor.

Table 4.12 : ANOVA Table for FF

Control Factors	Level (dB)			DF	SSQ	MSQ	Factor effect (%)	empty or pooled F=<1.5
	1	2	3					
Perovskite Thickness	34.84	34.98	34.49	2	0	0	1	pooled
TiO2 Thickness	34.80	34.64	34.87	2	0	0	0	pooled
Perovskite Donor Density	37.31	33.62	33.38	2	29	14	94	no
TiO2 Donor Density	35.13	34.97	34.22	2	1	1	5	pooled

Table 4.13 displays the selected levels based on their higher S/N ratios. The final step involves predicting and confirming the enhancement in performance characteristics using the chosen optimal levels of process parameters. The optimal S/N ratio achieved for the process parameters is 37.30 dB which aligns closely with the anticipated range value (38.21 dB to 36.40 dB). This prediction suggests improved performance characteristics with the selected optimal parameters.

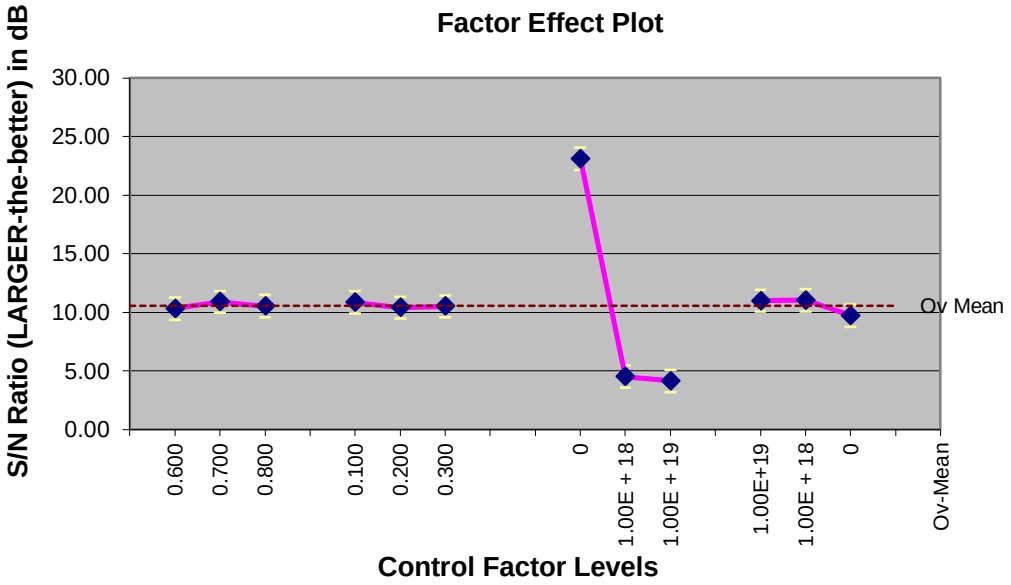

Figure 4.3: S/N Plot for FF

Table 4.13: S/N Ratio Prediction for FF

Control Factors	Level			Optimum Level	Factor effect (%)	Dominant, Significant or Neutral
	1	2	3			
Perovskite Thickness	0.600	0.800	0.700	2	1	Neutral
TiO2 Thickness	0.100	0.200	0.300	3	0	Neutral
Perovskite Donor Density	1E+17	1E+18	1E+19	1	95	Dominant
TiO2 Donor Density	1E+19	1E+18	1E+17	1	5	Neutral
S/N Ratio			37.30 dB			
	38.21 dB				36.40 dB	

4.4.3 Optimization of Voc in Tin Halide Perovskite Solar Cell

Table 4.14 presents the results for the open circuit voltage (VOC) in the PSC device using the L9 orthogonal array. Following the completion of the nine experiments within the L9 array, the next step is to determine the output values for the selected parameters, such as buffer thickness, buffer donor density, perovskite thickness, and perovskite donor density, which may influence the device's performance.

According to Table 4.15, a higher S/N ratio corresponds to a higher quality attribute. Table 4.15 shows the S/N ratios for the Voc experiment runs, adhering to the larger-the-better principle. The η for each experiment was calculated using Equation (3.12). The orthogonal array (OA) experimental design facilitates the separation of each parameter's effects on the S/N ratio at various levels. Table 4.16 provides an overview of the S/N ratio for each level of the control factors, as well as the total mean S/N ratio for the nine tests, along with the factor effect percentages.

Table 4.14: Voc Repetition Experiment Values

Exp No	Measurements for Each Experiment			
	1	2	3	4
1	6.06E-01	6.06E-01	5.99E-01	5.99E-01
2	1.03E-01	1.03E-01	1.03E-01	1.03E-01
3	1.02E-01	1.02E-01	1.03E-01	1.03E-01
4	1.04E-01	1.04E-01	1.04E-01	1.04E-01
5	1.03E-01	1.03E-01	1.03E-01	1.03E-01
6	6.12E-01	6.12E-01	6.04E-01	6.04E-01
7	1.03E-01	1.03E-01	1.03E-01	1.03E-01
8	6.20E-01	6.20E-01	6.12E-01	6.12E-01
9	1.04E-01	1.04E-01	1.04E-01	1.04E-01

Table 4.15: S/N Response for Voc

Mean Sum of Squares of reciprocals	SN Ratio (Larger-the-Better)
2.75E+00	-4.40
9.42E+01	-19.74
9.53E+01	-19.79
9.29E+01	-19.68
9.51E+01	-19.78
2.71E+00	-4.32
9.44E+01	-19.75
2.64E+00	-4.21
9.33E+01	-19.70

Table 4.16 : ANOVA Table for Voc

Control Factors	Level (dB)			DF	SSQ	MSQ	Factor effect (%)	empty or pooled F=<1.5
	1	2	3					
Perovskite Thickness	-14.64	-14.59	-14.55	2	0	0	0	pooled
TiO2 Thickness	-14.61	-14.58	-14.60	2	0	0	0	pooled
Perovskite Donor Density	-4.31	-19.71	-19.77	2	476	238	100	no
TiO2 Donor Density	-14.63	-14.60	-14.56	2	0	0	0	pooled

For the open-circuit voltage (Voc) of the PSC device, perovskite donor density (Factor C) accounts for 100% of the effect. In contrast, Factors A (perovskite thickness), B (TiO2 thickness), and D (TiO2 donor density) do not contribute any significant impact on Voc, as their factor effects are null. These three factors are considered pooled, meaning their levels contribute almost evenly and do not

significantly affect the design. Therefore, the levels for Factors A, B, and D can be selected as desired, since they have minimal impact. According to Table 4.16, the perovskite donor density (Factor C) is identified as the primary factor affecting Voc in this design. The analyzed performance improvement suggests that the optimal condition is A3B2C1D3.

Figure 4.4 illustrates the S/N Ratio (Larger-the-Better) graphs, where the dotted lines represent the total mean of the S/N ratio, and the diamond plots indicate the factor effects. The graph shows that control Factors A and D have approximately the same S/N value, while Factor B shows a slight change in S/N between its levels. Control Factor C displays the largest difference among its levels, with level 1 having the highest S/N ratio.

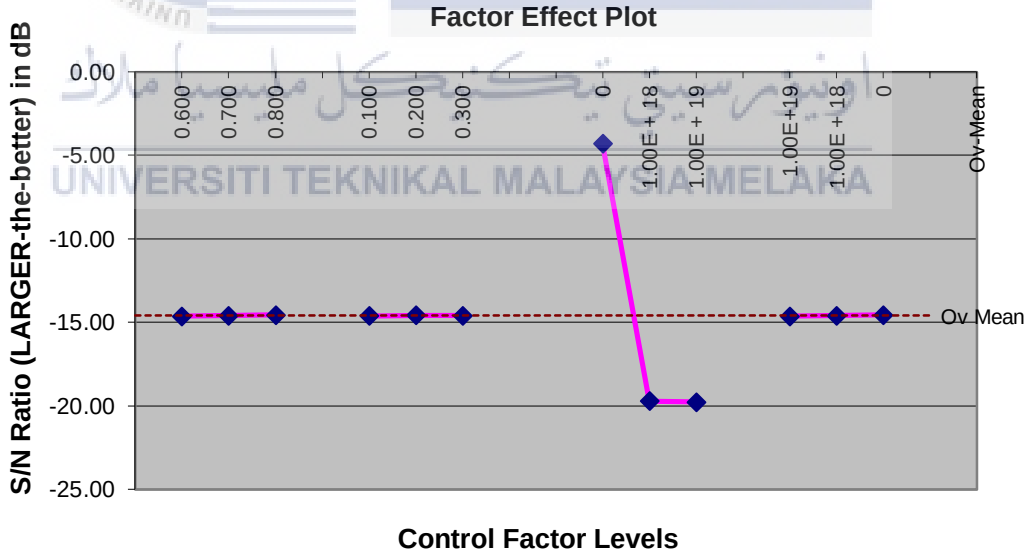

Figure 4.4: S/N Plot for Voc

Table 4.17 shows the levels selected based on their higher S/N ratios. After choosing the optimal level of the process parameters, the final step is to predict and verify the S/N ratio at the optimum level of the control factors. The S/N ratio at the optimum level of the process parameters is -4.3 dB, which is predicted to reflect the performance characteristics.

Table 4.17: S/N Ratio Prediction for Voc

Control Factors	Level			Optimum Level	Factor effect (%)	Dominant, Significant or Neutral
	1	2	3			
Perovskite Thickness	0.600	0.800	0.700	3	1	Neutral
TiO2 Thickness	0.100	0.200	0.300	2	0	Neutral
Perovskite Donor Density	1E+17	1E+18	1E+19	1	94	Dominant
TiO2 Donor Density	1E+19	1E+18	1E+17	3	5	Neutral
S/N Ratio	-4.30 dB					
	-4.20 dB				-4.42 dB	

4.4.4 Optimization of Jsc for Tin Halide Perovskite Solar Cell

Table 4.18 presents the results for the short-circuit current density (Jsc) in the PSC device using the L9 orthogonal array. Following the completion of nine experiments, with four trials for each experiment, the next phase is to determine the desired values for the respective control factors. Based on Table 4.19, a higher S/N ratio indicates better quality traits of the control factor. The orthogonal experiment design facilitates the selection by revealing the effect of each control factor on the S/N ratio across various levels. Using the L9 orthogonal array method in this experiment, it is possible to isolate the effect of each control factor on the S/N ratio at various levels.

Table 4.18 : Jsc Repetition Experiment Values

Exp No	Measurements for Each Experiment			
	1	**2**	**3**	**4**
1	3.21E+01	3.21E+01	3.21E+01	3.21E+01
2	3.33E+01	3.33E+01	3.36E+01	3.36E+01
3	3.32E+01	3.32E+01	3.32E+01	3.32E+01
4	3.39E+01	3.39E+01	3.40E+01	3.40E+01
5	3.39E+01	3.39E+01	3.40E+01	3.40E+01
6	3.26E+01	3.26E+01	3.26E+01	3.26E+01
7	3.44E+01	3.44E+01	3.45E+01	3.45E+01
8	3.11E+01	3.11E+01	3.11E+01	3.11E+01
9	3.43E+01	3.43E+01	3.43E+01	3.43E+01

Table 4.19 : S/N Respone for Jsc

Mean Sum of Squares of reciprocals	SN Ratio (Larger-the-Better)
9.68E-04	30.14
8.93E-04	30.49
9.07E-04	30.42
8.66E-04	30.62
8.66E-04	30.62
9.41E-04	30.26
8.43E-04	30.74
1.03E-03	29.86
8.51E-04	30.70

Table 4.20 lists the S/N ratios for each level of the process parameters. For the Jsc output in this PSC device design, the perovskite donor density (Factor C) is the most influential process parameter, accounting for 77% of the effect on device performance. According to Table 4.20, perovskite donor density was identified as the major factor affecting the performance of the perovskite cell, while the other control factors (A, B,

and D) had as minor factor affecting, each contributing less percentage. The analysis of average performance indicates that the optimal condition is A2B1C2D2.

Table 4.20: ANOVA Table for Jsc

Control Factors	Level (dB)			DF	SSQ	MSQ	Factor effect (%)	empty or pooled F=<1.5
	1	2	3					
Perovskite Thickness	30.35	30.50	30.43	2	0	0	5	no
TiO2 Thickness	30.50	30.32	30.46	2	0	0	8	no
Perovskite Donor Density	30.09	30.61	30.60	2	1	0	77	no
TiO2 Donor Density	30.49	30.50	30.30	2	0	0	11	no

The S/N Ratio (Larger-the-Better) graphs are shown in Figure 4.5, with factor effects represented by diamond plots and the total mean of the S/N ratio represented by dotted lines. As depicted in this graph, which is derived from Table 4.20, Factors A, B, and D all exhibit similar traits and do not impact the optimization process. Meanwhile, control factor C shows the most significant change in S/N ratio, indicating its importance in improving the devices short-circuit current. This graph indicates that the higher the level of the control factor with the highest S/N ratio (η), the more dominant the factor is. For instance, the thickness of the perovskite layer (Factor C) has the highest S/N Ratio (η) compared to other control factors at the same level of the total mean.

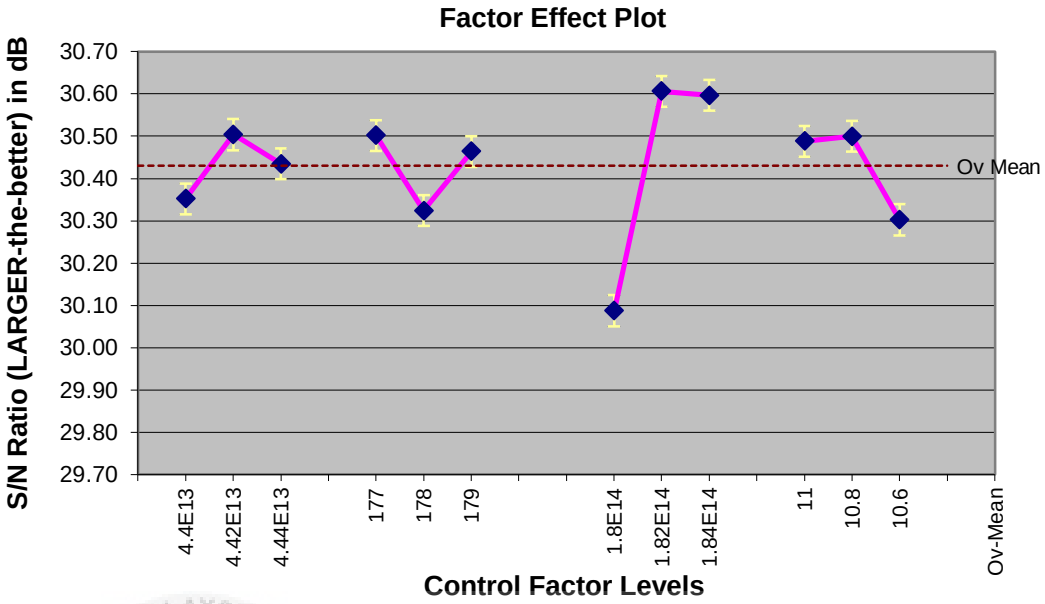

Figure 4.4: S/N Plot for Jsc

Table 4.21 shows the optimum level was selected based on their higher S/N ratios. After choosing the optimal level of the process parameters, the final step is to predict and verify the S/N ratio at the optimum level of the control factors. For the short-circuit current (Jsc), the thickness of the perovskite donor density (Factor C) was identified as the major factor affecting the Jsc in the device, with a 77% effect. In contrast, the other factors had a 5%, 8%, 11% or significant effect, indicating they were not neutral to the Jsc. The optimal S/N ratio for the significant control factor is 30.80 dB, which lies within the expected range (30.90 dB to 30.74 dB), thereby predicting the performance characteristics of this PSC device.

Table 4.21: S/N Ratio Prediction for Jsc

Control Factors	Level			Optimum Level	Factor effect (%)	Dominant, Significant or Neutral
	1	2	3			
Perovskite Thickness	0.600	0.800	0.700	2	5	Significant
TiO2 Thickness	0.100	0.200	0.300	1	8	Significant
Perovskite Donor Density	1E+17	1E+18	1E+19	2	77	Dominant
TiO2 Donor Density	1E+19	1E+18	1E+17	2	11	Significant
S/N Ratio			30.80 dB			
	30.90 dB				30.74 dB	

4.5 Multiple Optimization using Taguchi Method

Based on individual results from PCE, FF, JSC, and VOC, the average performance analysis for each parameter was conducted. The optimum levels were selected based on higher S/N ratios, indicating the most effective settings. The factor effect percentages on the S/N ratio highlight the dominant factors among the control factors. Table 4.22 displays the multiple optimization results derived from these analyses.

Based on the analysis from Table 4.22, each of the four control factor perovskite thickness (Factor A), TiO (Factor B), perovskite donor density (Factor C), and TiO2 donor density (Factor D), demonstrates varying degrees of influence on the Signal-to-Noise (S/N) ratio across the output parameters PCE, FF, Jsc, and Voc. Factor A, represented by perovskite thickness, was consistently selected at Level 2 despite its effect (5%) on the output parameters. This choice was made because Level 2 was optimized across three parameter PCE, FF, and Jsc. Factor B, TiO2 thickness, was uniformly chosen at Level 1 as it contributed optimally to all output parameters.

Factor C, perovskite donor density, emerged as the most influential factor across all parameters due to its dominant effect percentage. Level 1 was selected as optimal for Factor C, achieving 100% effectiveness for FF, while Level 1 optimized 99% for PCE and 94% for Voc. Similarly, Factor D, TiO2 donor density, saw Level 2 chosen as optimal, primarily due to its 11% effect on Jsc, making it the most significant level for this parameter.

Table 4.22: Multiple Optimization Table

Output Parameter	Measurements for Each Experiment				S/N Ratio (dB)	Value
	A	B	C	D		
PCE	2 (0%)	1(0%)	1(99%)	2 (0%)	23.1	27.11 %
FF	2 (0%)	3(0%)	1 **(100%)**	1 (0%)	37.30	86.12 %
Voc	3 (1%)	2(0%)	1(94%)	3 (5%)	-4.3	0.967 V
Jsc	2 **(5%)**	1 **(89%)**	2 (77%)	2 **(11%)**	30.80	33.82 mA/cm²
Multiple Optimization	**2**	**1**	**1**	**2**		

The S/N ratios reflect the performance of each parameter under the optimized experimental conditions, confirming the final values achieved for each output parameter. Notably, Factor C (perovskite donor density) emerges as the most critical control factor, significantly influencing the optimization of the tin halide perovskite device across multiple parameters. Ultimately, after thorough optimization across all output parameters, the optimal design configuration identified for the PSC device is A2B1C1D2. This selection reflects the culmination of efforts to enhance device performance through strategic control of process parameters, guided by rigorous experimental design and analysis.

From the description, Table 4.23 presumably displays the values of each parameter both before and after optimization. The TiO2 thickness remains unchanged before and after optimization, indicating its stability in the experimental setup. In contrast, factors A, C, and D are likely referring to perovskite donor density, perovskite thickness, and TiO2 donor density, respectively were optimized from Level 3 to Level 3. This adjustment aligns with the application of the larger-the-better principle in the research, aiming to enhance the electrical parameters and observe substantial improvements across all output parameters: PCE, FF, Voc, and Jsc.

Table 4.23: Final Optimization Parameters

Control Factors	Initial Parameter	Optimized Parameter
Perovskite Thickness	0.700	0.800
TiO2 Thickness	0.100	0.100
Perovskite Donor Density	1.00E+19	1.00E+17
TiO2 Donor Density	1.00E+ 18	1.00E+19

Table 4.24 highlights the optimization results for PCE, FF, Voc and Jsc, where significant increases are observed in these output parameters following individual optimizations, while Voc remains unchanged. However, during multiple optimizations, it becomes evident that PCE and Jsc values increase, whereas FF and Voc values decrease. This trade-off reflects the inherent compromise required to enhance the efficiency of the design by improving some parameters at the expense of others. The multiple optimization approach demonstrates that maximizing PCE and Jsc while accepting decreases in FF and Voc represents the optimal strategy for enhancing this mixed halide perovskite device. Overall, the optimized outcomes across all output parameters surpass those reported in previous research journals.

Table 4.24: Before and after Optimization Comparison

Parameters	Before Optimization	After Optimization		Previous Journal [2]
		Individual	Multiple	
PCE (%)	26.24	27.10	27.11	25.26
FF (%)	84.22	86.12	86.11	84.05
J_{sc} (mA/cm^2)	21.23	33.82	33.82	18.15
V_{oc} (V)	0.97	0.97	0.97	0.95

CHAPTER 5

CONCLUSION AND FUTURE WORKS

This chapter will discuss the overall conclusion by providing the overall summary of the project. Future works on the improvement that can be made will also be suggested.

5.1 Conclusion

This project aimed to design and optimize tin halide perovskite solar cells (PSCs) using computational modeling and experimental analysis. The primary objectives were to utilize SCAPS-1D software for designing efficient tin halide PSCs and to analyze their performance characteristics.

The initial phase focused on utilizing SCAPS-1D software to simulate and design tin halide PSCs. This computational approach allowed for the exploration of optimal material compositions and device configurations, providing insights into the electrical and optical properties critical for achieving high efficiency.

Following the design phase, experimental optimization was conducted to enhance the performance of tin halide PSC devices. By systematically varying parameters such as perovskite thickness and composition, the study aimed to improve device efficiency and stability under varying environmental conditions.

The analysis of tin halide PSC efficiency revealed promising results, indicating significant progress in enhancing device performance through computational design and experimental optimization. This research contributes to the ongoing efforts in advancing perovskite solar cell technology, focusing on improving efficiency, stability, and scalability for future sustainable energy applications.

In conclusion, this project underscores the potential of tin halide perovskite materials in renewable energy technology and highlights the importance of integrating computational modeling with experimental validation to accelerate advancements in solar cell efficiency and performance. Future research directions will continue to explore novel materials, device architectures, and fabrication techniques to further optimize tin halide PSCs for commercial viability and widespread adoption.

5.2 Future Works

Perovskite solar cells commonly incorporate lead in their structure, which can emit harmful gases during chemical processes, contributing to environmental pollution. This issue highlights concerns regarding the toxicity and environmental impact associated with these cells. Researchers are actively exploring alternatives that are lead-free and developing eco-friendly fabrication techniques to ensure the sustainability of perovskite technology.

Perovskite solar cells are versatile, capable of being manufactured on flexible substrates, enabling the production of lightweight, flexible, and even transparent solar panels. Ongoing research aims to improve the mechanical durability and efficiency of large-area and flexible perovskite solar cells for applications such as wearable electronics, building-integrated photovoltaics (BIPV), and portable power generation.

Despite achieving high power conversion efficiencies (PCEs) exceeding 27%, perovskite solar cells continue to offer opportunities for improvement. Scientists are investigating new materials, engineering methods, and device architectures to enhance efficiency further and address challenges such as charge recombination and limitations in light absorption. Optimizing the composition, structure, and interfaces of perovskite materials holds potential for significant increases in efficiency.

Perovskite solar cells can also be combined with other solar cell technologies, such as silicon or thin-film solar cells, to create tandem or multi-junction devices. These configurations can achieve higher efficiencies by utilizing a broader spectrum of sunlight, optimizing wavelength absorption, and maximizing energy conversion efficiency. Developing efficient and stable tandem configurations involving perovskite solar cells alongside materials like silicon or organic semiconductors remains an active area of research.

REFERENCES

[1] M. M. Haque et al., “Study on the interface defects of eco-friendly perovskite solar cells,” Sol. Energy, vol. 247, no. April, pp. 96–108, 2022.

[2] P. Roy, N.K. Sinha, A. Khare, “Progress in efficiency and stability of hybrid perovskite photovoltaic devices in high reactive environments,” in: Hybrid Perovskite Compos. Mater., Elsevier, pp. 239–257, 2021.

[3] D. Maradin, “Advantages and disadvantages of renewable energy sources utilization,” Int. J. Energy Econ. Policy, vol. 11, no. 3, pp. 176–183, 2021.

[4] A. M. Titu, A. V. Sandu, A. B. Pop, S. Titu, and T. C. Ciungu, “The Taguchi Method Application to Improve the Quality of a Sustainable Process,” IOP Conf. Ser. Mater. Sci. Eng., vol. 374, no. 1, 2018.

[5] S. Pitchaiya et al., “A review on the classification of organic/inorganic/carbonaceous hole transporting materials for perovskite solar cell application,” Arab. J. Chem., vol. 13, no. 1, pp. 2526–2557, 2020.

[6] E. Widianto, Shobih, E. S. Rosa, K. Triyana, N. M. Nursam, and I. Santoso, "Performance analysis of carbon-based perovskite solar cells by graphene oxide as hole transport layer: Experimental and numerical simulation," Opt. Mater. (Amst)., vol. 121, 2021.

[7] A. K. Kadhim, M. R. Mohammad, and A. I. Abd Ali, "Enhancing the efficiency of perovskite solar cells by modifying perovskite layer with rGO additive," Chem. Phys. Lett., vol. 786, no. November 2021, p. 139189, 2022.

[8] S. Rai, B. K. Pandey, and D. K. Dwivedi, "Modeling of highly efficient and low cost CH3NH3Pb(I1-xClx)3 based perovskite solar cell by numerical simulation," Opt. Mater. (Amst)., vol. 100, no. December 2019, p. 109631, 2020.

[9] N. Aggarwal and S. K. Sharmar, "Optimization of process parameters by Taguchi based Grey Relational Analysis," Int. J. Curr. Eng. Technol., vol. 4, no. 4, pp. 2792–2796, 2018.

[10] M. F. Hossain, M. Faisal and H. Okada, "Device Modeling and Performance Analysis of Perovskite Solar Cells Based on Similarity with Inorganic Thin Film Solar Cells Structure," 2016 2nd International Conference on Electrical, Computer & Telecommunication Engineering (ICECTE 2016), pp. 1-4, 2016.

[11] M. S. Jamal, S. A. Shahahmadi, M. A. A. Wadi, P. Chelvanathan, N. Asim, H. Misran, M. I. Hossain, N. Amin, K. Sopian and M. Akhtaruzzaman, "Effect of defect density and energy level mismatch on the performance of perovskite solar

cells by numerical simulation," International Journal for Light and Electron Optics, vol. 182, pp. 1204–1210, Elsevier 2019.

[12] M. K. S. Rafiq, M. Akhtaruzzaman, K. S. Rahman and M. T. Ferdaous, "A Comprehensive Defect Study of Tungsten Disulfide (WS2) as Electron Transport Layer in Perovskite Solar Cells by Numerical Simulation," Results in Physics, vol. 12, pp. 1097-1103, 2019.

[13] R. Katiyar, A. Kumar and B. S. Sengar, "Numerical simulation of highefficient perovskite-based solar cells using SCAPS 1D," 2020 5th International Conference on Emerging Electronics (ICEE 2020), New Delhi, India, pp. 1-4, 2020.

[14] S. Nair, S. B. Patel and J. V. Gohel, "Recent trends in efficiency-stability improvement in perovskite solar cells," Materials Today Energy, vo. 17, p. 100449, Elsevier 2020.

[15] Phadke MS., "Quality Engineering Using Robust Design," Pearson Education, Inc. and Dorling Kindersley Publishing, Inc., 1998.